ACADEMIA ROMÂNĂ
Revue Roumaine de Chimie
http://web.icf.ro/rrch/

Rev. Roum. Chim.,
2012, *57*(4-5), 521-529

Dedicated to Professor Ionel Haiduc
on the occasion of his 75th anniversary

ICOSAHEDRAL AlMnLn (Ln = Ce, Gd, Dy, Ho) ALLOYS – AN EXAFS STUDY AND CATALYTIC BEHAVIOR

Simona M. COMAN,[a] Dan MACOVEI[b] and Vasile I. PÂRVULESCU[a,*]

[a] Department of Organic Chemistry, Biochemistry and Catalysis, Faculty of Chemistry, University of Bucharest, 4-12 Regina Elisabeta Bdv., 030016 Bucharest, Roumania
[b] National Institute of Materials Physics, 105bis Atomistilor Str., PO Box MG. 7, Magurele-Bucharest, 077125, Roumania

Received August 22, 2011

Two series of icosahedral $Al_{100-x-y}Mn_xLn_y$ alloys, first consisting of AlMnCe with variable Ce (x = 6 and y = 1, 2, 3, 4: $Al_{93}Mn_6Ce$, $Al_{92}Mn_6Ce_2$, $Al_{91}Mn_6Ce_3$, and $Al_{90}Mn_6Ce_4$) or Mn (x = 8, 10; y = 1: $Al_{89}Mn_{10}Ce$ and $Al_{91}Mn_8Ce$) concentration, and the second consisting of constant alloy composition ($Al_{91}Mn_6Ln_3$), while varying the Ln nature (Gd, Dy, and Ho) were prepared. The icosahedral structure of the samples was confirmed by X-ray diffraction (XRD). As shown by EXAFS, the sample $Al_{89}Mn_{10}Ce$, with the lowest Ce/Mn ratio, display an advanced degree of disorder around the Ce atoms in the structure. Catalytic behavior highly depended on the alloys structure, the higher the degree of disorder around the rare-earth element in the structure, the higher catalytic activity. Replacing Ce with Gd, Dy or Ho in AlMnLn alloys does not result in a significant enhancement of the catalytic performances.

INTRODUCTION

Aluminium alloys with transition metals (TM) are extensively used in industry due to their specific advantages, like low mass density, mechanical performances, structural flexibility, relatively simple processing, and low costs compared with other light materials. Depending on the chemical composition or the processing way, Al-TM alloys with nano-crystalline, nano-icosahedral (quasicrystalline) or amorphous structure can be prepared. The quasicrystalline structure, discovered by Shechtman[1] in Al-Mn alloys, is an aperiodic well-ordered structure, but with long-range positional order instead of the translational order characteristic of the periodic, crystalline lattices. In particular, the icosahedral quasicrystals have twofold, threefold and fivefold rotational axes, defining the icosahedral symmetry.

Adding rare earths elements (Ln) to Al-TM alloys considerably improves their thermal stability (e.g., up to 300-350°C comparing with 150-200°C, characteristic for the conventional Al alloys), preserving their mechanical properties up to relatively high temperatures.[2-3] The Al-TM-Ln alloys have also icosahedral structure and their preparation requires non-equilibrium techniques, like ultrafast solidification of the melt (10^5-10^6 $K \cdot sec^{-1}$). RE presence in the composition of the melted Al-TM alloy increases the viscosity of the melt, slowing down the crystallisation of equilibrium phases and favouring the quenching of the metastable configurations of the liquid state.[4] However, due to the relatively high atom mobility, a high quenching rate is essential for the icosahedral-phase formation. The Al-TM-Ln alloys prepared in this way consist of icosahedral nano-particles dispersed in the Al matrix.[5] Inclusion of

* Corresponding author: vasile.parvulescu@g.unibuc.ro

the large-size Ln atoms in the Al-TM alloys can influence specific changes of their structure, not always well known. Knowledge of the local configurations around the RE atoms and their locating in the Al-TM-Ln structure could contribute to a better description of these materials.

The potential application of quasicrystals for catalysis was first investigated by Nosaki et al.[6] Latter, Tsai and coworkers[7-10] studied the catalytic properties of icosahedral quasicrystal systems from Al–Cu–Fe alloys with various compositions for the steam reforming reaction of methanol. Some fundamental studies of adsorption and/or reactivity of simple molecules (*e.g.*, CO, CH_3OH and H_2) on the surface of quasicrystals such as Al–Pd–Mn,[11-12] Al–Ni–Co[13] and Ti–Zr–Ni[14] were also reported. They also suggested excellent hydrogenation properties.

This study discusses an EXAFS characterization of icosahedral Al-Mn-Ln (Ln = Ce, Gd, Dy, Ho) alloys prepared by a melt-spinning technique and their catalytic behavior in styrene hydrogenation.

RESULTS AND DISCUSSION

The Fourier transforms (FT) of EXAFS, calculated for the AlMnCe alloys, are shown in Fig. 1. Except $Al_{89}Mn_{10}Ce$, the FT's are practically identical for all the samples, pointing out similar atomic configurations around Ce. The first main maximum of each FT, corresponding to the nearest neighbouring shell of Ce, was isolated and back-transformed into the *k*-space. The resulting spectra $k^3\chi_1(k)$ (Fig. 2) describe the contribution to EXAFS from the nearest neighbours of Ce, filtered out of the experimental EXAFS.

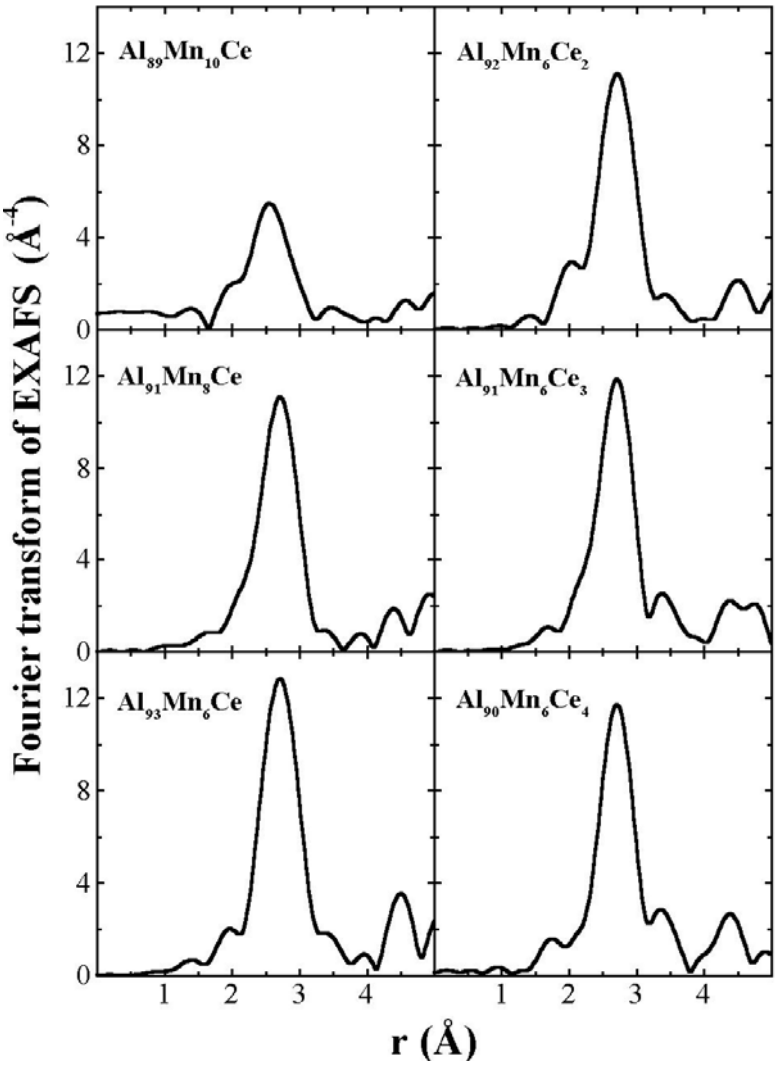

Fig. 1 – Fourier transforms of the experimental $k^3\chi(k)$ spectra of the i-AlMnCe alloys.

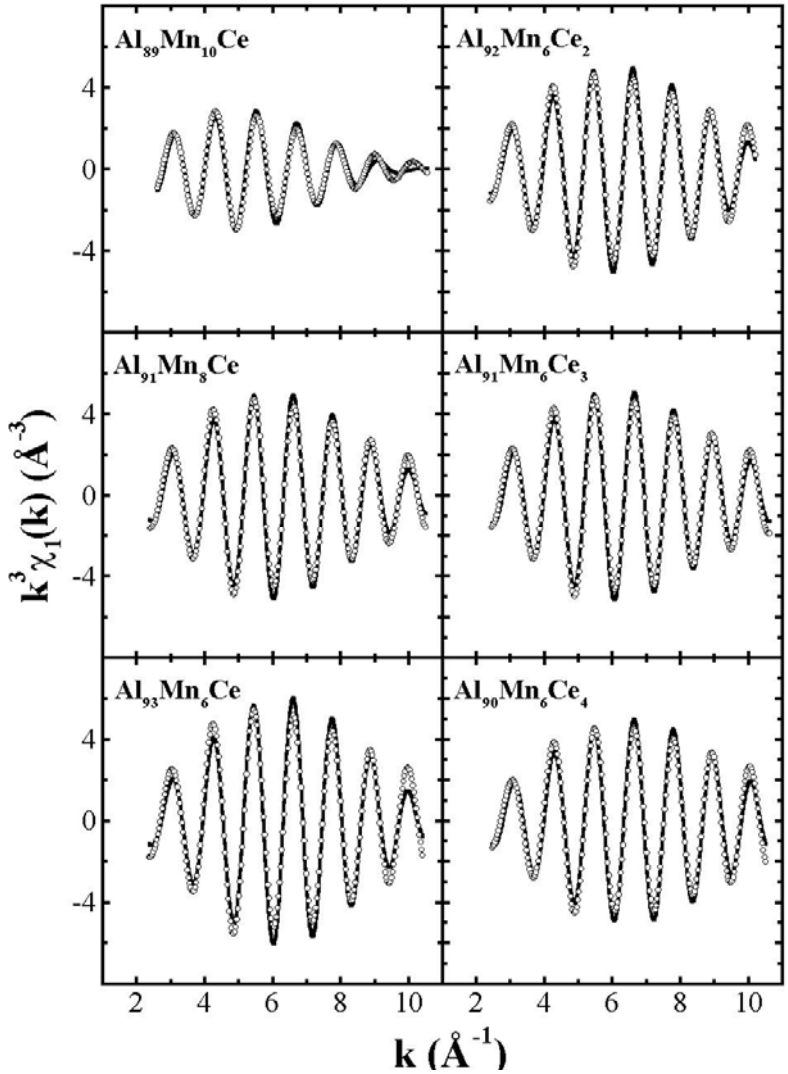

Fig. 2 – The filtered $k^3\chi_1(k)$ spectra (—) of the i-AlMnCe alloys and their fit (○○○) with Mn and Al nearest neighbours.

The filtered $k^3\chi_1(k)$ spectra were successively fitted with an unique Al neighbouring shell, a split shell of Al neighbours, at two different average distances, and a split (Mn, Al) shell. The fit with the Al shell was very poor, whereas its split in two Al sub-shells improved the quality of the fit, but resulted in abnormally short Ln-Al distances. The best fit was systematically that with Mn and Al nearest neighbours (Table 1).

As shown by EXAFS, the sample $Al_{89}Mn_{10}Ce$, with the lowest Ce/Mn ratio, behaves differently with respect to the other samples. The high values of the Debye-Waller factors (σ^2) point out an advanced degree of disorder around the Ce atoms in the structure of this sample. The numbers of the nearest neighbours and the interatomic Ce-Mn and Ce-Al separations are also smaller than the corresponding values for most of the other AlMnCe alloys. The peculiar structure around Ce at this composition is due to the prevalent Ce location in the Al matrix, instead of the icosahedral phase. Determinations by transmission electron microscopy and energy dispersive X-ray spectrometry (not shown here) found for this sample about 80% of Ce being diluted in an Al-rich matrix, without forming the icosahedral alloy. Therefore, most of the EXAFS signal comes from this Ce fraction, prevailing over the contribution of Ce in the icosahedral structure.

The FT's of experimental EXAFS and the filtered $k^3\chi_1(k)$ spectra of the samples $Al_{91}Mn_6Ln_3$, with Ln = Gd, Dy and Ho, are shown in Figs. 3 and 4, respectively. As in the case of the i-AlMnCe alloys, the best fit of the filtered EXAFS was that with Mn and Al neighbours. The results of the fit are indicated in Table 2, together with those obtained for $Al_{91}Mn_6Ce_3$.

Table 1

Ce environment in the i-AlMnCe alloys

Sample	Ce/Mn	*N*	*R* (Å)	σ^2 ($x10^{-3}$ Å^2)
$Al_{89}Mn_{10}Ce$	0.10	1.6 Mn 7.5 Al	2.85 3.17	12 16
$Al_{91}Mn_8Ce$	0.12	2.2 Mn 8.9 Al	2.91 3.20	9 8
$Al_{93}Mn_6Ce$	0.17	2.0 Mn 8.8 Al	2.91 3.21	5 5
$Al_{92}Mn_6Ce_2$	0.33	1.6 Mn 8.4 Al	2.91 3.21	6 6
$Al_{91}Mn_6Ce_3$	0.50	2.1 Mn 9.2 Al	2.91 3.17	9 7
$Al_{90}Mn_6Ce_4$	0.67	1.4 Mn 7.5 Al	2.91 3.19	4 5

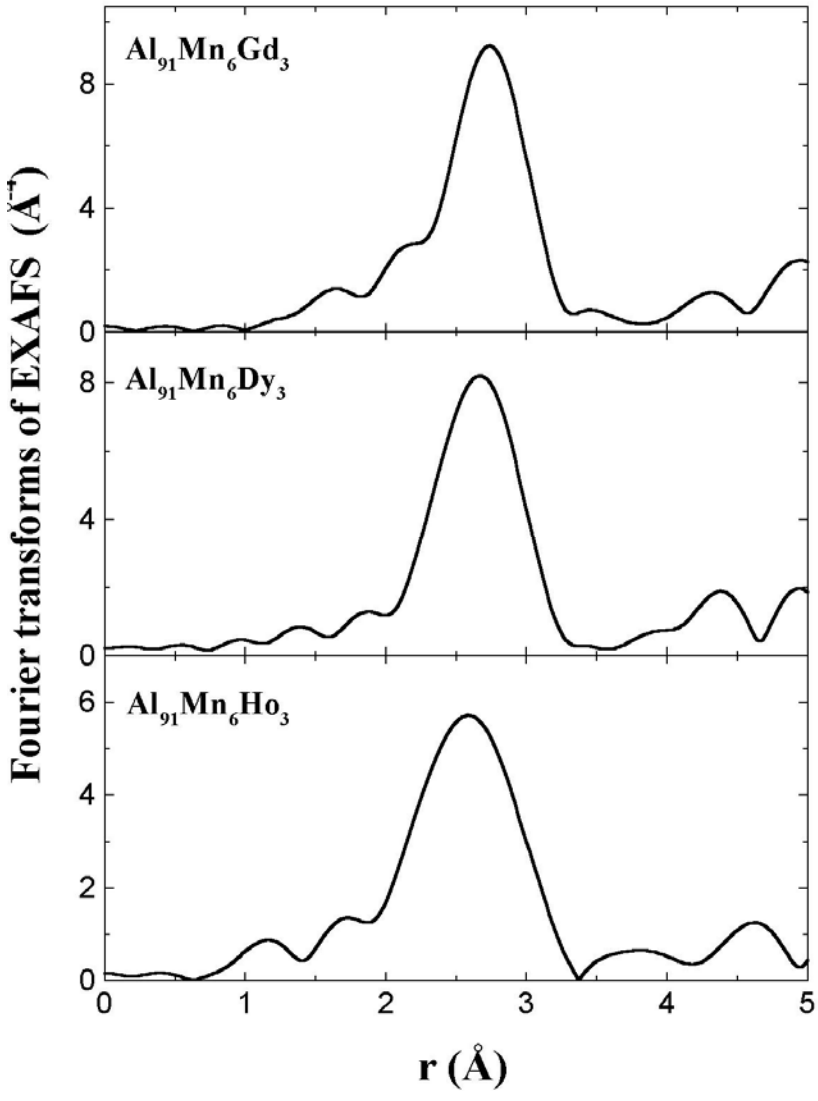

Fig. 3 – Fourier transforms of the experimental $k^3\chi(k)$ spectra of the i-$Al_{91}Mn_6Ln_3$ (Ln = Gd, Dy, Ho) alloys.

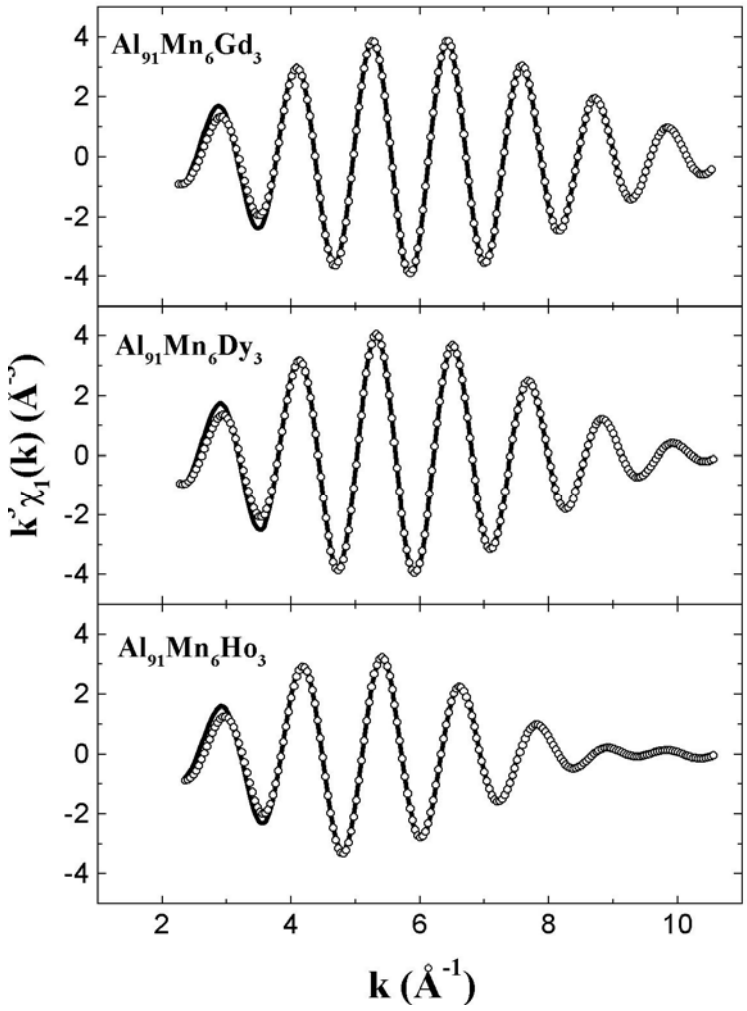

Fig. 4 – The filtered $k^3\chi_1(k)$ spectra (—) of the i-$Al_{91}Mn_6Ln_3$ alloys and their fit (○○○) with Mn and Al neighbours.

Table 2

Ln environment in the i-$Al_{91}Mn_6Ln_3$ (Ln = Ce, Gd, Dy, Ho) alloys

Sample	*N*	*R (Å)*	σ^2 *(x10^{-3} Å^2)*
$Al_{91}Mn_6Ce_3$	2.1 Mn 9.2 Al	2.91 3.17	9 7
$Al_{91}Mn_6Gd_3$	1.3 Mn 8.8 Al	2.91 3.20	8 10
$Al_{91}Mn_6Dy_3$	1.6 Mn 8.9 Al	2.85 3.17	9 11
$Al_{91}Mn_6Ho_3$	2.0 Mn 8.5 Al	2.77 3.13	15 15

One can observe a close similarity of the Ln environment between alloys with various Ln's, with the numbers of Mn and Al neighbours varying in the narrow ranges 1.6-2.1 and 8.5-9.2, respectively. The slight decrease of the Ln-Mn and Ln-Al distances in the Ln sequence Ce, Gd, Dy, Ho is related to the decrease of the metallic Ln radius in the same sequence (1.82 Å, 1.80 Å, 1.78 Å, and 1.76 Å, respectively).

The Ln environment in i-$Al_{91}Mn_6Ln_3$ with the local surroundings of Al and non-Al atoms in two types of icosahedral quasicrystals, with simple icosahedral (SI) and face-centred icosahedral (FCI) structures was also compared.

Table 2

Ln environment in the i-$Al_{91}Mn_6Ln_3$ (Ln = Ce, Gd, Dy, Ho) alloys

Sample	*N*	*R (Å)*	σ^2 *(x10^{-3} Å^2)*
$Al_{91}Mn_6Ce_3$	2.1 Mn 9.2 Al	2.91 3.17	9 7
$Al_{91}Mn_6Gd_3$	1.3 Mn 8.8 Al	2.91 3.20	8 10
$Al_{91}Mn_6Dy_3$	1.6 Mn 8.9 Al	2.85 3.17	9 11
$Al_{91}Mn_6Ho_3$	2.0 Mn 8.5 Al	2.77 3.13	15 15

One of the most studied SI quasicrystals is the i-AlMnSi ($Al_{73}Mn_{21}Si_6$) alloy. Its structure was described by a quasi-periodic arrangement of icosahedral structural units $Mn_{12}(Al,Si)_{42}$,[15-16] known as Mackay icosahedra (MI). Similarly to i-AlMnSi, i-AlMn has a SI structure, with a P-type hyperlattice in 6D.[17] Rare-earth adding could preserve this structure or could change it to FCI symmetry. It is worth noting that some icosahedral MgZnLn alloys, with Ln = Dy, Er, Ho, and Tb, were found to possess a FCI structure,[18-19] but also SI structure for Ln= Er, Ho, and Tm, and at a higher Zn/Mg ratio.[20] In several cases, the Ln presence favours the FCI structure. Al substitution by Ho or Er in MgZnAl alloys changes the SI structure of the host into a FCI structure, with a chemical ordering of Ln on certain specific sites of the quasilattice.[21]

Knowledge of the Ln environment in i-AlMnLn should help to discern between the SI and FCI types of its structure. The obtained EXAFS results on Ln surrounding, averaged over the $Al_{91}Mn_6Ln_3$ samples with Ln = Ce, Gd, Dy, and Ho, are given in Table 3. In the icosahedral structure of $Al_{91}Mn_6Ln_3$, the average Ln environment consists of 1.8 Mn and 8.9 Al nearest neighbours, at 2.86 Å and 3.17 Å, respectively. These results were compared with previous EXAFS studies of the local structure around Al in SI AlMnSi[22] and around *non*-Al atoms in FCI AlCuFe and AlCuRu.[23]

As found by Sadoc[22], the Al atoms in i-AlMnSi are closely surrounded by 2.5 Mn and 9.4 Al neighbours at the distances 2.54 Å and 2.78 Å, respectively. The authors found a similar Al environment in crystalline α-AlMnSi, as a consequence of the same building blocks (Mackay icosahedra) in the atomic structures of i-AlMnSi and α-AlMnSi. Comparison of these results with the Ln environment in i-AlMnLn indicates a simple-icosahedral structure of these quasicrystals. The Ln inclusion in the SI AlMn quasilattice did not change, at least for the studied composition, the host symmetry.

Although the Ln environment in AlMnLn is closely related to that of Al in i-AlMnSi, the interatomic distances around Ln are lengthened by 0.3-0.4 Å (see Table 3), with respect to the distances around Al in AlMnSi. This structure expansion is due to the changes resulting by the accommodation of the voluminous Ln atoms in the AlMn structure. The distance elongation is approximately the same as the difference between the metallic radii of the Ln atoms, ranging between 1.76 Å (Ho) and 1.82 Å (Ce), and the radius of Al (1.43 Å).

The catalytic activity results (overall reaction rate and selectivity) using the investigated AlMnCe alloys are shown in Table 4. The overall reaction rates have been calculated using equation 1.[24]

$$\int_0^X \frac{dX}{(-r')} \approx \frac{X}{(-r')}(Xsmall) \Rightarrow (-r') = \frac{F_0 X}{W} \qquad \text{Eq. 1}$$

Conversions smaller than 12% justify the differential reactor assumption. Recent contributions suggested working even at more severe limits, below 5 percent.[24] However, the contribution of the errors in these measurements exists always, like in all the calculations referring to the kinetics in heterogeneous catalysts. The main source of errors results from the precision of the way the data used to carry out the calculations is collected. In this study they have been measured using chromatographic analysis, and the typical error of this kind of measurements is in between 5 and 10%. To avoid the contribution of the errors we have repeated five times the experiments using fresh catalysts and the values presented in Table 1 represent the average of these measurements.

Under these conditions the differences in the calculus of the reaction rate were smaller than 5% that correspond to the level of exigency for such kind of calculations. The calculated values are in the typical range reported for noble metal supported catalysts.

The advantages using these catalysts are however important. They replace expensive noble metal species and as alloy ribbons are less sensible to manipulation. The alloy state is also removing any mass transfer limitation. Data presented in Table 4 also show the effect of the alloy composition. The catalysts from the second series showed superior reaction rates compared with the catalysts from the first series, suggesting that an increased content of manganese exhibits a positive effect. On the other side, the increase of the cerium content exhibits a detrimental effect as it can be observed from the results obtained for the second series. These results are well correlated with the disorder around the Ce atoms and the interatomic Ce-Mn and Ce-Al separations determined from EXAFS measurements. Fig. 5 depicts the overall rate against the Ce/Mn ratio. The increase of the cerium content led to a decrease of the reaction rate. As shown by EXAFS, in the samples with the lowest Ce/Mn ratio, Ce is prevalent located in the Al matrix, instead of the icosahedral phase. The presence of manganese as a very close neighbour of aluminium in these materials is also in line with the variation presented in Fig. 5. This very good correlation demonstrates that the active site is an arrangement generated in the Al matrix by the combination of manganese and cerium.

The presence of Ln elements (Ln = Gd, Dy, and Ho) occurs especially in the icosahedral AlMnLn phase and in consequence was found to exhibit almost no catalytic effect.

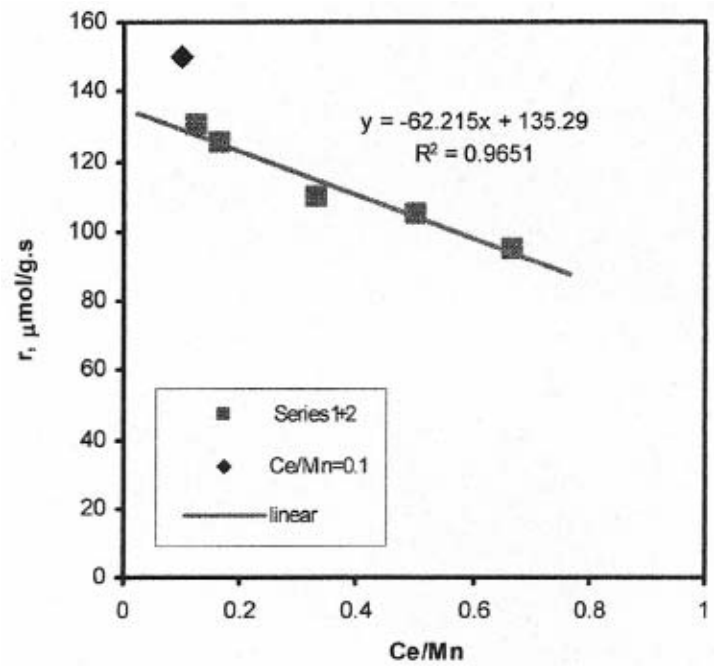

Fig. 5 – Plot of the overall rate against Ce/Mn ratio.

Table 4

Catalytic activity of AlMnCe alloys at 70ºC and 0.5 mL/min H_2

Catalyst	Ce/Mn	$r_{styrene}$ µmol/g s	Ethylbenzene/ethylcyclohexane ratio
$Al_{89}Mn_{10}Ce$	0.10	150	1/0
$Al_{91}Mn_{8}Ce$	0.12	130	1/0
$Al_{93}Mn_{6}Ce$	0.17	125	1/0
$Al_{92}Mn_{6}Ce_{2}$	0.33	110	1/0
$Al_{91}Mn_{6}Ce_{3}$	0.50	105	1/0
$Al_{90}Mn_{6}Ce_{4}$	0.67	95	1/0

The data presented in the same Table 4 showed that at these low conversions and temperature the selectivity to ethylbenezene was 100% irrespective to the icosahedral alloy composition. However, increasing the conversion to over 85% and reaction temperature to 90 ^{o}C the oligomerization of styrene was also observed with a decrease of the selectivity to around 90%.

EXPERIMENTAL

Nano-icosahedral Al-Mn-Ln alloys were prepared by a melt-spinning technique. Primary alloys of various nominal compositions, obtained from high-purity metals, were first melted under Ar atmosphere. The melt was then ultrafast quenched on the surface of a copper wheel rotating at 2500 rpm. The resulting samples were ribbons of about 1-mm width and 35-μm thickness.

Two series of icosahedral $Al_{100-x-y}Mn_xLn_y$ alloys were prepared. The first one consisted of AlMnCe samples with variable Ce concentration (x = 6 and y = 1, 2, 3, 4: $Al_{93}Mn_6Ce$, $Al_{92}Mn_6Ce_2$, $Al_{91}Mn_6Ce_3$, and $Al_{90}Mn_6Ce_4$) or Mn concentration (x = 8, 10; y = 1: $Al_{89}Mn_{10}Ce$ and $Al_{91}Mn_8Ce$). The nominal Ce/Mn ratio in the sample composition ranged between 0.10 ($Al_{89}Mn_{10}Ce$) and 0.67 ($Al_{90}Mn_6Ce_4$). For the other series, the alloy composition was constant ($Al_{91}Mn_6Ln_3$), while varying the Ln nature (Gd, Dy, and Ho). The icosahedral structure of the samples was confirmed by x-ray diffraction. As found by electron microscopy, the alloys consisted of icosahedral AlMnLn nano-particles highly dispersed in al Al-rich matrix.

EXAFS was measured at the Ln-L_3 edges. The primary absorption spectra were measured in transmission mode at Beijing Synchrotron Radiation Facility, at energies between 250 eV below the Ln L_3 edge and 450 eV (Ce) or 650 eV (Gd, Dy, Ho) above. The energy separation in the EXAFS range was about 3 eV.

For the data analysis, the pre-edge background of the spectra was calculated by its fitting with Victoreen formula, and subtracted from the spectra. The EXAFS function $\chi(k)$ (k = photoelectron wavevector) was calculated by normalizing the absorption oscillations in the EXAFS range to the structureless atomic absorption. The latter one was approximated by the post-edge background of the spectrum, fitted by polynomial cubic splines. The $k^3\chi(k)$ spectra were Fourier inverted over the k range 2.0-10.9 Å^{-1} (Ce) or 2.0-13.1 Å^{-1} (Gd, Dy, Ho), resulting in radial functions with maxima corresponding, up to systematic shifts, to the neighbouring shells of the Ln atoms. The first main maximum of the Fourier transforms was isolated by Hanning windows and back-transformed into k space. The so filtered EXAFS spectrum $k^3\chi_1(k)$, describing the nearest neighbouring shell, was non-linearly fitted with one-shell and two-shell models, by a least-square method. The fit provided the number N of the nearest neighbours of the Ln atoms, interatomic Ln-neighbour distances (R), and the mean-square distance fluctuation (σ^2) in the nearest neighbouring shell of Ln. The electron backscattering amplitudes and phase shifts were calculated by the FEFF6 code.[25]

Catalytic tests were carried out at atmospheric pressure in an isothermal quartz flow reactor. Molecular hydrogen was bubbled inside the flask with mantle containing the styrene reactant at 70 ºC. The resulted mixture was preheated and introduced into the reactor (containing 1g of catalyst) with a flow rate between 0.5 and 2.0 ml/min. The control of temperature was kept with a thermostat. The reaction temperature was kept at 70ºC with a control of 0.5 ºC. The overall reaction rate was calculated based on the assumption of the differential reactor. It thus was calculated from the variation of the conversion as a function of the contact time for conversions smaller than 12%. The analysis of the products of the reaction was performed by GC-FID chromatografy (GC-Shimatzu aparatus in following conditions: column: CP-SIL 8 CB, 30 m, ID = 0.25 mm). The identification of the products was made using a GC-MS Carlo Erba Instruments QMD 1000 equipped with a Factor Four VF-5HT column with the following characteristics: 0.32mm x 0.1 μm x 15 m working with a temperature program at a pressure of 0.38 Torr with He as the carrier gas.

CONCLUSIONS

The comparison of the Ln environment in i-AlMnLn with that of Al in i-AlMnSi is somehow surprising, since the Ln atoms seem to be equivalent to Si, rather than to Al atoms in i-AlMnSi. Nevertheless, no differentiation between Al and Si sites in the icosahedral structure of AlMnSi has yet been reported. Although i-AlMnSi is a ternary quasicrystal, its structural models are actually binary (Al,Si)Mn models, with the Si atoms randomly distributed over Al sites. Therefore, the Ln atoms in the i-AlMnLn structure are equally equivalent to Al and Si atoms in i-Al(Si)Mn. This also means that the Ln and Al atoms occupy same type of sites in the simple-icosahedral structure of the AlMnLn quasicrystals.

The catalytic behavior of the quasicrystals alloys correlates with the disorder around the Ce atoms and the interatomic Ce-Mn and Ce-Al separations determined from EXAFS measurements: the higher the degree of disorder around Ce, the higher was the catalytic activity. The content in manganese is controlling the structure of icosahedral alloys. Thus, in the series of AlMnCe the highest activity was displayed by the $Al_{89}Mn_{10}Ce$ alloy. The presence of Ln elements (RE = Gd, Dy, and Ho) in AlMnLn alloys exhibited no catalytic effect.

REFERENCES

1. D. Shechtman, I. Blech, D. Gratias and J. W. Cahn, *Phys. Rev. Lett.*, **1984**, *53*, 1951-1953.

2. A. Inoue, Y. Yokoyama and T. Masumoto, *Mater. Sci. Eng. A,* **1994**, *181-182*, 850-855.
3. A. Inoue, H.M. Kimura and K. Kita, "New Horizons in Quasicrystals. Research and applications", A.I. Goldman, D.J. Sordelet, P.A. Thiel and J.M. Dubois (Eds.), World Scientific, Singapore, 1997, p. 256.
4. A. Inoue, K. Ohtera and T. Masumoto, *Jap. J. Appl. Phys.,* **1988**, *27*, L 736.
5. A. Inoue, *Nanostructured Materials*, **1995**, *6*, 53-64.
6. K. Nosaki, T. Masumoto, K. Inoue and T. Yamaguchi, US Patent 5800638, Sept. 1, 1998.
7. M. Yoshimura and A. P. Tsai, *J. Alloys Compd*., **2002**, *342*, 451-454.
8. A. P. Tsai and M. Yoshimura, *Appl. Catal. A,* **2001**, *214*, 237-241.
9. T. Tanabe, S. Kameoka and A. P. Tsai, *Catal. Today*, **2006**, *111*, 153-157.
10. M. Yamasaki and A. P. Tsai, *J. Alloys Compd*., **2002**, *342*, 469-472.
11. C. J. Jenks and P. A. Thiel, *J. Mol. Cat. A: Chemical*, **1998**, *131*, 301-306.
12. C. J. Jenks, T. A. Lofrasso and P. A. Thiel, *J. Am. Chem. Soc.,* **1998**, *120*, 12668-12669.
13. R. McGrath, J. Ledieu, E. J. Cox, C. J. Jenks and T. A. Lofrasso, *J. Alloys Compd*., **2002**, *342*, 432-436.
14. A. Sadoc, E. H. Majzoub, W. T. Huette and K. F. Kelton, *J. Alloys Compd*., **2003**, *356-357*, 96-99.
15. V. Elser and C.L. Henley, *Phys. Rev. Lett.*, **1985**, *55*, 2883-2886.
16. J. W. Cahn, D. Gratias and B. Mozer, *Phys. Rev. B*, **1988**, *38*, 1638-1642.
17. M. Mihalkovič, W. J. Zhu, C. L. Henley and R. Phillips, *Phys. Rev. B*, **1996**, *53*, 9021-9045.
18. A. Langsdorf and W. Assmus, *J. Cryst. Growth*, **1998**, *192*, 152-156.
19. I. R. Fischer, Z. Islam, A. F. Panchula, K. O. Cheon, M. J. Kramer, P. C. Canfield and A. I. Goldman, *Phil. Mag. B*, **1998**, *77*, 1601-1615.
20. E. Uhrig, S. Brühne, R. Sterzel, L. Schröpfer and W. Assmus, *Phil. Mag. Lett.*, **2003**, *83*, 265-272.
21. Z. Luo, S. Zhang, Y. Tang and D. Zhao, *Scripta Metall*., **1993**, *28*, 1513-1518.
22. A. Sadoc, A. M. Flank and P. Lagarde, *Phil. Mag. B*, **1988**, *57*, 399-410.
23. A. Sadoc, C. Berger and Y. Calvayrac, *Phil. Mag. B*, **1993**, *68*, 475-479.
24. M. E. Davis and R. J. Davis, "Fundamentals of Chemical Reaction Engineering", McGraw-Hill, New York, 2003, p. 87.
25. J. J. Rehr, J. Mustre de Leon, S. I. Zabinsky and R. C. Albers, *J. Am. Chem. Soc.*, **1991**, *113*, 5135-5140.